Gas Transport Properties of Liquid Crystalline Poly(*p*-phenyleneterephthalamide)

D. H. Weinkauf, H. D. Kim,† and D. R. Paul*

Department of Chemical Engineering and Center for Polymer Research, The University of Texas at Austin, Austin, Texas 78712

Received July 22, 1991; Revised Manuscript Received October 3, 1991

ABSTRACT: A series of films were prepared from anisotropic poly(*p*-phenyleneterephthalamide) (PPT) solutions and annealed at 100, 200, and 300 °C. By using cross polarized light microscopy, the PPT films appeared to exhibit a completely anisotropic morphology. From X-ray diffraction analysis, each of the films appeared to contain a fixed level of modification II crystallites with the level of modification I crystallites increasing with annealing temperature. Amorphous films were also prepared from a structural isomer of PPT which contains a large fraction of meta linkages along the polymer main chain. Permeability measurements were made for He, H_2, O_2, N_2, and CO_2 at 35 °C and the diffusivities of the larger gases were computed from time-lag data. In general, the permeability coefficients of the PPT films are very low and approach those reported for poly(acrylonitrile) (PAN) and liquid crystalline copolyesters. The oxygen permeability coefficients of the amorphous PPT isomer are over 1 order of magnitude larger than those for the anisotropic PPT materials. The solubility coefficients for the noncrystalline regions of the PPT and PPT isomer, however, are very close. In contrast with the well-documented effect of meta- versus para-linked moieties on transport in amorphous, glassy polymers, the mesomorphic para-linked PPT materials exhibit oxygen diffusion coefficients that are nearly 1 order of magnitude lower those of the meta-linked PPT isomer. Among the PPT films, the permeability coefficients of the samples annealed at 100 and 200 °C are nearly the same, while annealing at 300 °C results in significant reductions in both permeability and diffusivity.

Introduction

Most studies of sorption and diffusion of small molecules in polymers have dealt with totally amorphous materials.[1,2] For semicrystalline polymers, the usual physical picture employs a two-phase model with all diffusion occurring in the amorphous phase since the crystals are generally thought to be impermeable.[3,4] Although recently, evidence of sorption and diffusion of gases in very loosely packed polymer crystals has been presented.[5] The mesophase of liquid crystalline polymers (LCP) may be thought of as a third state that could be useful in the development of unique membrane or barrier materials. In any case, it is likely that the nature of this state can be better understood by sorption and diffusion observations. As suggested in Figure 1, the mesomorphic structure of a liquid crystalline phase has a degree of order between that of amorphous and crystalline phases. In previous papers, thermotropic liquid crystalline copolyesters have been shown to exhibit excellent gas barrier properties stemming from the extraordinarily low solubility of gases in these materials.[6-8] Given the rigid nature of these polymer chains and their efficient packing, low permeabilities are not surprising. However, low permeability usually stems from low mobility of the penetrant in the polymer matrix rather than low solubility. A survey of conventional polymers shows that the solubility coefficient for a gas like oxygen rarely varies by more than a factor of 5 even when the permeability varies by orders of magnitude. The objective of this paper is to compare the gas transport properties of an aromatic polyamide LCP with those observed for thermotropic copolyesters having varying levels of aromatic character. The polymer selected, poly(*p*-phenyleneterephthalamide) (PPT) is a commercial product that has been the subject of considerable fundamental interest.

Poly(*p*-phenyleneterephthalamide) is not thermotropic and must be solution processed, i.e., lyotropic. It is spun from liquid crystalline solutions to form high modulus Kevlar fibers.[9] The highly crystalline morphology and excellent physical properties of the finished Kevlar fibers have been well documented.[10-12] Films from PPT solutions have also been fabricated and characterized in a few laboratories.[13-16] The crystalline structure is described as paracrystalline.[12] The effects of the type of coagulant and of annealing temperature on the crystal structure of PPT films have been extensively examined by Haraguchi et al.[14,15]

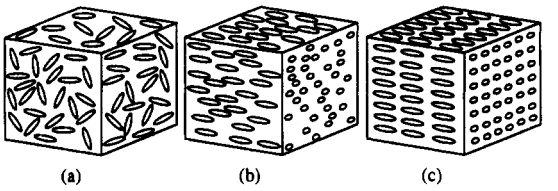

Figure 1. Schematic diagrams of (a) isotropic, (b) mesomorphic, and (c) fully crystalline arrangements of elliptical molecules.

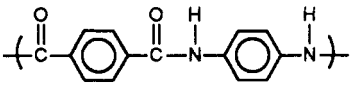

PPT

The well-documented high water sorption capacity of polyamides such as Nylon 6 and 6,6 has been linked closely with the concentration of amide linkages along the polymer chain.[17] Despite crystallinity levels near 75%, Kevlar fibers have also been observed to absorb appreciable amounts of water.[18] Unlike Nylon 6 and 6,6 materials, the polymeric chains in Kevlar fibers have no isotropic character.[10] Thus, it appears as though the ordered (but noncrystalline) regions of the Kevlar fibers behave analogously to the amorphous regions of other polyamides. If this is a characteristic of isotropic and mesomorphic arrangements of chemically similar polymer chains, then one would also expect similar behavior with other penetrants including simple gases.

The following structural isomer of PPT forms a completely amorphous material and allows for a reasonable

* Author to whom correspondence should be addressed.
† Permanent address: Department of Textile Engineering, College of Engineering, Pusan National University, Pusan 609-735, Korea.

0024-9297/92/2225-0788$03.00/0

comparison of the effect of mesomorphic order on the transport properties:

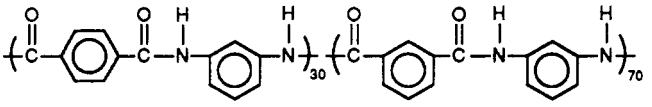

The structure is similar to that incorporated in Du Pont's Nomex fibers and will be referred in the text as the PPT isomer. Differences in transport properties between meta- and para-linked isomers that form amorphous, glassy polymers are most often manifested in the diffusivity of a penetrant;[19-23] therefore, one would expect that the solubility behavior would be relatively unaffected except by issues concerning the ordering of the polymer chains and subsequent loss of free volume.

This paper reports gas transport measurements made on a series of films prepared from liquid crystalline PPT solutions and several other conventionally processed polyamides including the PPT isomer. By changing the annealing temperature, the level of crystallinity in the PPT films could be significantly changed, which allowed the effect of this variable on permeation to be investigated. Observations using crossed polarized light experiments confirm that the PPT films are nearly 100% anisotropic, thus, the remaining noncrystalline regions apparently exist as a glassy mesophase. Extensive analysis of the crystalline structure and complex morphology of the films provided necessary complementary information for interpreting the gas transport measurements.

Background

The issues of chemical structure, chain rigidity, and level of crystallinity are essential for understanding of the gas transport properties of the PPT films. Therefore, it will be useful to briefly describe the elements of the solution–diffusion mechanism for gas transport in polymers. This model is stated in terms of permeability, solubility, and diffusivity coefficients, i.e.

$$P = DS \tag{1}$$

The diffusion coefficient, D, is associated with the degree of penetrant mobility in the polymer and is lower the stronger the cohesive forces between chains and the more efficiently the polymer chains are packed together (i.e., low free volume available for diffusion). The solubility coefficient, S, is thermodynamic in nature and is determined by the condensibility of the gas, the interactions with the polymer, and to some extent the free volume available in the polymer matrix.

The effect of crystallinity on the permeation in polymers is most often described by a two-phase model for transport.[3,4] The degree of chain packing in most conventional polymeric crystallites effectively prohibits the dissolution of even small gas molecules. Consequently, the reduced equilibrium solubility coefficient in semicrystalline polymers is effectively related to the volume fraction of crystalline phase, X_c, by[3,4]

$$S = S_{nc}(1 - X_c) \tag{2}$$

where S_{nc} is the solubility coefficient for the completely noncrystalline material. This model has proved useful over a wide range of crystallinity levels for several polymer systems.[3,4]

The effective diffusion coefficient decreases with increasing crystallinity because of the reduction in space available for diffusion and the longer or more tortuous path that the penetrant must take in order to get around the impermeable regions. The length of the effective diffusional path is highly dependent upon the shape and arrangement of the impermeable phase, thus attempts to correlate the crystalline volume fraction and effective diffusivity have had more limited success.[24-26] As a first and probably underestimated approximation, a relationship similar to that for solubility has been found adequate for some polymer systems.[24,25] Equations 2 and 3 combined

$$D = D_{nc}(1 - X_c) \tag{3}$$

with eq 1 give an estimate of the effect of crystallinity on permeability. Although generally applied to systems of crystalline and amorphous phases, the two-phase model will be a useful preliminary guage to differentiate the effects of the fully crystalline phase from those of the anisotropic noncrystalline regions.

Experimental Section

Materials and Film Preparation. A series of films that differ only in annealing conditions were prepared from commercial Du Pont Kevlar 49 fibers. The as-received fibers were washed in acetone, rinsed in distilled water, and then dissolved in 99.8% sulfuric acid to form an 11 wt % polymer solution at room temperature. The dope was gold in color and highly birefringent when observed under crossed polarizers indicating a high degree of local anisotropy in the PPT solution. The dope was cast onto glass plates at room temperature with the aid of a casting blade and then coagulated by rinsing thoroughly in distilled water. After subsequent washing steps with a 0.1% $NaOH_3$ solution and, again, with distilled water, the films were placed between two absorbent blotters with moderate pressure overnight to remove residual water from the samples. The films were removed from the sandwich of blotters and then annealed for 2 h at the various temperatures while being held lightly between the platens of a compression molder.

The structural isomer of PPT described above was also obtained from Du Pont. Amorphous films were prepared by casting from a 5 wt % solution of dimethylacetamide (DMAc, bp = 166 °C) onto glass plates in a vacuum oven. The temperature in the oven was ramped over a period of several days to 150 °C. The films were then freely suspended in the vacuum oven and held at 150 °C for 2 weeks. The temperature of the oven was then increased above the glass transition temperature (245 °C) to 310 °C and held for several more days. At this drying temperature, the color of the films turned amber apparently indicating some degree of thermal degradation. However, the toughness of the films was not significantly compromised suggesting that the molecular weight remained high. According to thermal gravimetric analysis (TGA), all residual DMAc in the PPT isomer films was effectively removed in the final drying step.

For comparitive analysis of transport properties, films were also prepared from two commercial polyamides, poly(6-aminohexanoic acid) (Nylon 6) obtained from Allied Signal Corp and poly(*m*-xyleneadipamide) (MXD6) obtained from Mitsubishi Gas Chemical Co. The Nylon 6 and MXD6 materials were dried for several days under vacuum at 90 °C and then compression molded at a temperature 20 °C above their respective melting points of 225 and 235 °C. A moderately fast quenching step limited the crystallinity levels to near 25% in both of the samples as deduced from analysis of the enthalpies of melting using DSC.

Property Measurement. The permeability coefficients, P, of a series of pure gases were measured at 35 °C using the standard transient permeation technique employed in this laboratory.[27] The upstream driving pressures were 5 atm for helium, hydrogen, and oxygen, 10 atm for carbon dioxide, and 15 atm for nitrogen. Effective diffusion coefficients were estimated from the film thickness, l, and the time lag, θ, using[28]

$$D = l^2/6\theta \tag{4}$$

Time-lag values ranged from several seconds for helium to 20 h for the larger gases like nitrogen and carbon dioxide. The

apparent solubility coefficient, S, for each gas was estimated by dividing the permeability coefficient by the diffusion coefficient as suggested by eq 1.

Wide-angle X-ray diffraction patterns were obtained using a Philips automatic diffractometer utilizing Cu Kα radiation (λ = 1.54 Å) arranged in the reflection mode. X-ray photographs were also taken with a flat-plate camera set up in the transmission mode using the same radiation source. Photographs were taken with the beam normal to the film surface (through view) as well as 90° off normal (edge view) to provide information about any preferred orientation of the lattice planes.

Thermal analysis was conducted on a Perkin-Elmer Model 7500 thermal analyzer equipped with both DSC and TGA. The DSC scans were conducted at a rate of 20 °C/min. The amount of sorbed water in the PPT samples was estimated by observing weight loss using TGA. Samples from each film were ramped from 25 to 600 °C at 10 °C/min. Degradation became evident at temperatures near 450 °C, and all samples were reduced to a black char upon reaching 600 °C.

Bulk densities of the films were measured by two methods. The first was a density gradient column based on degassed aqueous calcium nitrate solutions at 25 °C. The densities of several samples from each film were recorded. In each case, replicate values fell within 0.001 g/cm^3 of the average reported for each of the samples. Because of the tendency for water sorption in PPT materials,[18] we were concerned about the validity of the absolute values obtained in the aqueous density gradient column even though reproducibility was good. Thus, as an alternative the densities were also measured by a floatation method in toluene–carbon tetrachloride solutions. Solutions having densities in the range of interest were prepared by titrating toluene (ρ = 0.866 g/cm^3) into a flask containing carbon tetrachloride (ρ = 1.586 g/cm^3). The range of titrated solutions were calibrated with glass beads of known density. At each incremental density, the samples were allowed to float or sink after thorough mixing. The accuracy of this method was roughly estimated to be ±0.005 g/cm^3.

Results and Discussion

Film Characterization. The physical properties of the aromatic polyamide films used in this study are given in Table I. The thickness of the PPT films were near 1.0 mil (25 μm), while those for the PPT isomer varied from 1 to 4 mil depending upon casting conditions. The color of the PPT films ranged from gold to golden-brown with increased annealing temperature. Under crossed polarizers, the PPT films were highly birefringent suggesting that the anisotropy observed in the dope was preserved during film formation and annealing. Films of the PPT isomer showed no birefringence and, thus, were thought to be truly amorphous. The photomicrographs of the PPT films shown in Figure 2, made using crossed polarizers, indicate that rather dramatic morphological changes occur as annealing temperature is increased. The grainy texture of the sample annealed at 100 °C is gradually replaced with fairly distinct opaque domains. The domains in the sample annealed at 300 °C appear to have a spherulitic or hedritic texture; however, their density and thickness prevent the transmission of light and more concise characterization. Since decomposition accompanies the melting phenomenon in these materials near 500 °C, the levels of crystallinity could not be measured through analysis of the heats of fusion.

Crystalline Structure. The crystalline structure of PPT films has been found to be dependent on the coagulant used during film formation.[14] Films coagulated from water form a less thermally stable crystalline lattice termed modification II, whereas most other coagulants result in the formation of modification I type crystallites.[14] Figures 3 and 4 show X-ray diffraction photographs of the films with the beam normal and perpendicular to the film surface, respectively. The diffuse nature of the reflections

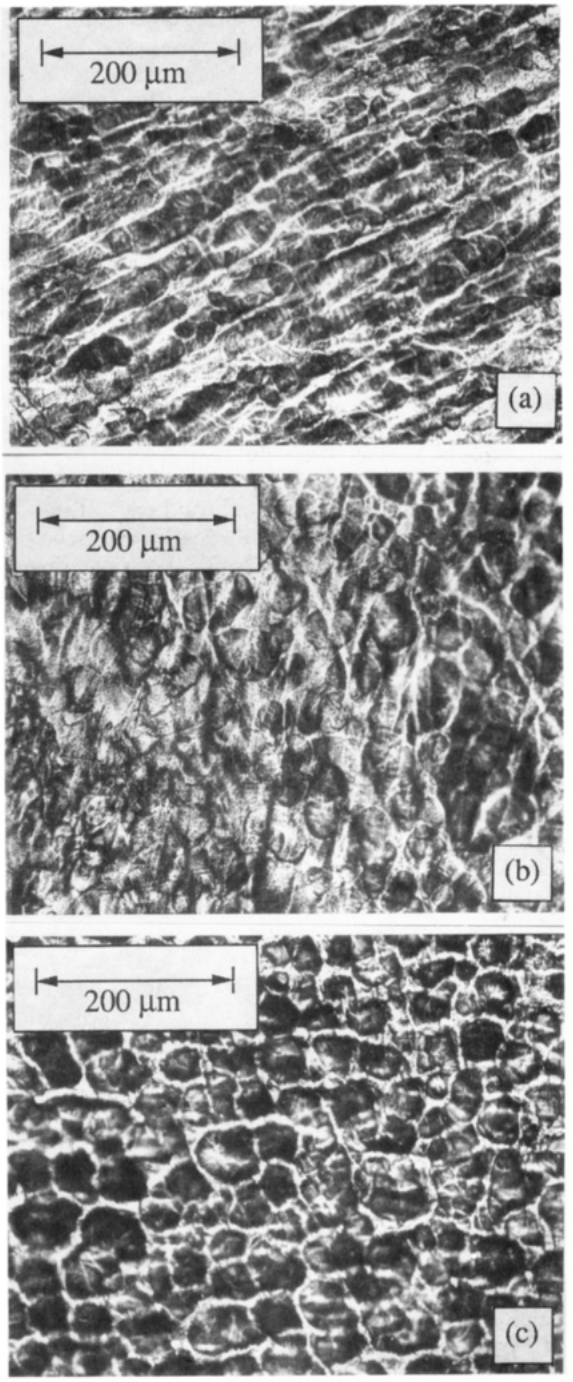

Figure 2. Photomicrographs of (a) PPT-100, (b) PPT-200, and (c) PPT-300 films using cross polarized light.

is characteristic of the paracrystalline structure expected for these samples. From the "through view" projections in Figure 3, the complete halos correspond to the (200) and (004) lattice reflections of the pseudoorthorhombic crystal structure.[12,14] The complete halos indicate that the a–c planes of the crystals are randomly oriented with respect to the axis normal to the film surface. The "edge view" photographs, however, show that some preferred orientation exists. The dominant (010) reflection, or "inner" reflection, on the meridian in the edge view photographs is a fingerprint of the modification II type crystal structure.[14] Although difficult to quantify from the photographs in Figure 4, the relative intensity of the "inner" reflection to the (200) reflection along the meridian appears to diminish with increased annealing temperature suggesting that new crystals are being formed with their a axis normal to the film surface.

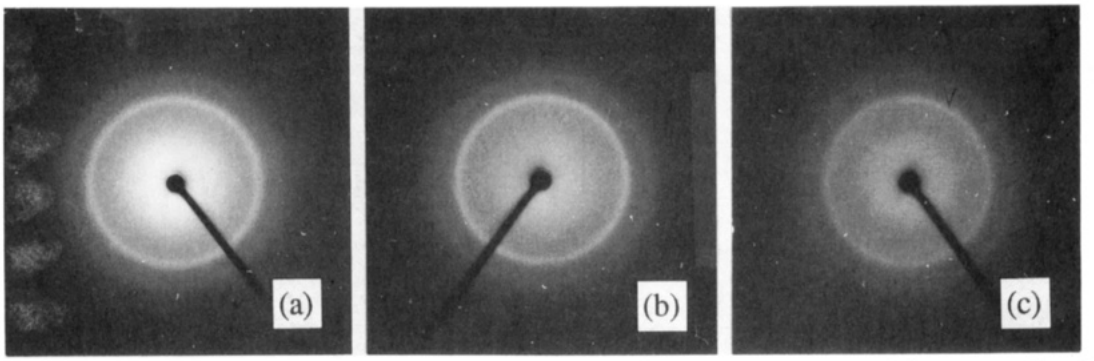

Figure 3. X-ray diffraction photographs for (a) PPT-100, (b) PPT-200, and (c) PPT-300 films with beam normal to film surface (through view).

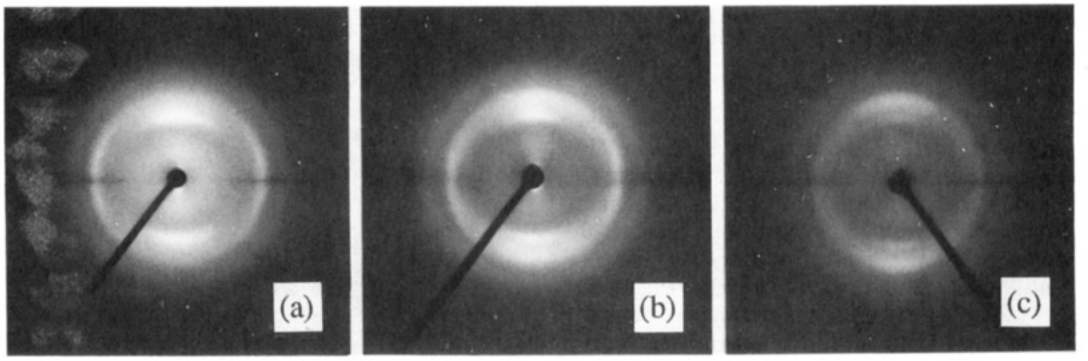

Figure 4. X-ray diffraction photographs for (a) PPT-100, (b) PPT-200, and (c) PPT-300 films with beam 90° off normal to film surface (edge view). Note shadow of film along the equator of the diffraction pattern.

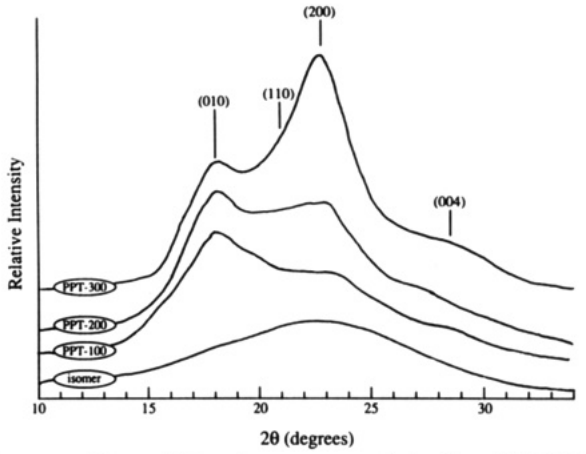

Figure 5. X-ray diffraction patterns of the three PPT films showing the effect of increased annealing temperature on the intensities of the various crystalline reflections in relation to the amorphous pattern of the PPT isomer.

The X-ray diffraction scans for the three annealed PPT films and the amorphous pattern of the structural isomer shown in Figure 5 allow a more graphic demonstration of the crystalline structural changes that take place during annealing. The intensity of the peak at $2\theta = 17.5$ associated with the (010) reflection in modification II type crystals remains constant over the range of annealing temperatures. The growth in intensity of the broad peak at $2\theta \approx 22$ results from an increase in periodicity of both the (200) and (110) reflections of modification I type crystals. Apparently, a certain amount of modification II type crystals are formed during initial film formation. These crystals are thermally stable over the range of annealing conditions used and are not transformed to modification I. However, during the annealing process and additional water removal, modification I type crystals are readily formed from the anisotropic but noncrystalline regions. These results are consistent with the those of Haraguchi et al. for the annealing of films which were prepared from solutions above the critical concentration for anisotropic phase formation.[14]

Level of Crystallinity. Determining the level of crystallinity in the PPT materials is made difficult by the disordered nature of the paracrystalline structure. The diffraction patterns in Figure 5 clearly show that the level of three-dimensional order in the PPT samples increases with annealing temperature. As outlined by Alexander,[29] the fraction of crystalline material, X_c, in polymeric materials can be approximated by

$$X_c = \int_{s_0}^{s_1} s^2 I_c(s)\, ds \Big/ \int_{s_0}^{s_1} s^2 I(s)\, ds \qquad (5)$$

where s is the radial distance in reciprocal space, or 2 sin θ/λ, while I and I_c represent the scattering intensity from the bulk sample and crystalline regions, respectively. A reasonable approximation of the noncrystalline scatter can be obtained from the amorphous diffraction pattern of the structural isomer of PPT. Intensity data for the crystalline scatter is then obtained by simply subtracting the noncrystalline scatter from the total or bulk diffraction pattern. The integrated intensities were calculated with the limits of integration, s_0 and s_1, of 0.225 and 0.744 (i.e. 10 and 35° 2θ). The crystallinity levels for the PPT-100, -200 and -300 samples were estimated to be 22, 38, and 45%, respectively. These estimates for the absolute crystallinity levels are rough since the nature of the paracrystalline structure, preferred orientation, and the use of an estimated noncrystalline scattering pattern severely limit the accuracy of this method. By applying the same method to the diffraction patterns of finely cut Nomex and Kevlar 49 fibers, the level of crystallinity in the Kevlar fibers was deduced to be 65%. Using similar but more accurate analysis of the fiber diffraction patterns, previous investigators have determined the level of crystallinity in Kevlar 49 fibers to be 75%.[11]

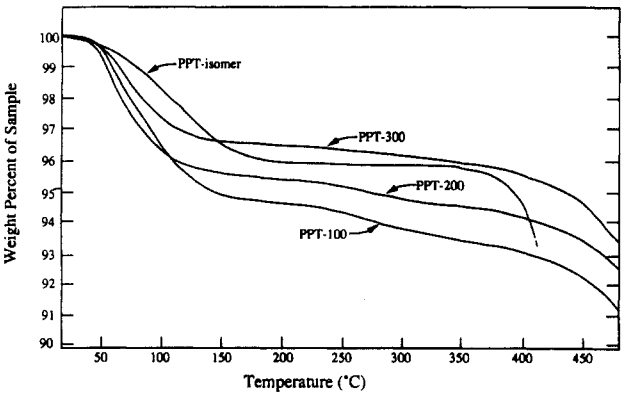

Figure 6. Percentage of initial sample weight versus temperature from thermogravimetric analysis (TGA) showing the relative water loss in the PPT and PPT isomer samples.

Sorbed Water and Density. As seen in Figure 6, TGA indicates a dramatic weight loss in all of the PPT materials between 50 and 150 °C including that of the PPT isomer. The weight loss has been attributed to the liberation of sorbed water molecules. These percentages are not unusual considering that the highly crystalline Kevlar 49 fibers have been observed to absorb as much as 8 wt % water.[18] Ambient relative humidity during this study was certainly high enough to account for these levels of water sorption. The water content in the PPT films decreases with increased annealing temperature. This trend could be expected owing to the increased volume fraction of crystallites deduced from the X-ray diffraction patterns. Curiously, however, the amount of sorbed water in the amorphous PPT isomer films is in the same range as that of the highly crystalline PPT materials suggesting that these materials have a similar equilibrium water sorption capacity.

The evolution of water from the samples is also made apparent by the broad endotherms near and above 100 °C in each of the DSC thermograms (Figure 7a). By dividing areas of these endothermic peaks by the heat of vaporization of water (40.65 kJ/mol), estimates for residual water content were obtained that are in approximate agreement with those deduced from TGA. After heating to 400 °C, second DSC traces show no evidence for evolution of sorbed species (Figure 7b). The glass transition temperature in the PPT isomer does not change between the first and second heating ramps indicating that the presence of water does not plasticize the material to any significant extent. The notable absence of a glass transition in the PPT materials in this temperature range is further evidence of the highly ordered nature of the films.

To ascertain how much water is present in the films during the permeation measurements, PPT film samples were carefully weighed and then placed in the permeation cell and degassed for two weeks at 35 °C. The mass of the PPT-100, -200, and -300 samples decreased by 3.9, 3.0, and 2.0 wt %, respectively. These amounts are equivalent to roughly 50–60% of the total sorbed water observed in TGA. The samples regained their original mass on exposure to ambient temperature and humidity for several weeks.

The densities of the films obtained by both experimental methods are given in Table I. The densities of the PPT films fall below the value of 1.440 g/cm^3 found for highly crystalline Kevlar 49 fiber but well above that of the amorphous PPT isomer. Agreement of the values obtained by the two methods was very good with the exception of the sample annealed at 100 °C. Densities measured on samples dried in the permeation cell described earlier were only slightly higher suggesting that the sorbed water only minimally affects the observed density. The change in density with degassing is not large enough to affect the general trend seen in Table I. Despite the higher crystallinity levels observed in the sample annealed at 200 °C, the density of the PPT-200 sample is consistently lower than that of the PPT-100 sample. As evidenced by crossed polarized light microscopy and X-ray diffraction, annealing at temperatures above 100 °C brings about the onset of rather dramatic morphological changes in the PPT films. Although the changes in the crystalline structure can be identified, the nature of the changes in the noncrystalline regions are more difficult to characterize. A number of morphological changes during annealing may be responsible for the unusual trend in densities. These include water loss, chain rearrangement in the noncrystalline regions, initial crystallization of more densly packed regions, and possibly the formation of microvoids during crystallization.

The high densities of the PPT materials suggest that the films are truly dense; however, the potential for some microvoiding in the PPT systems is a concern since this could have a very dramatic effect on the transport

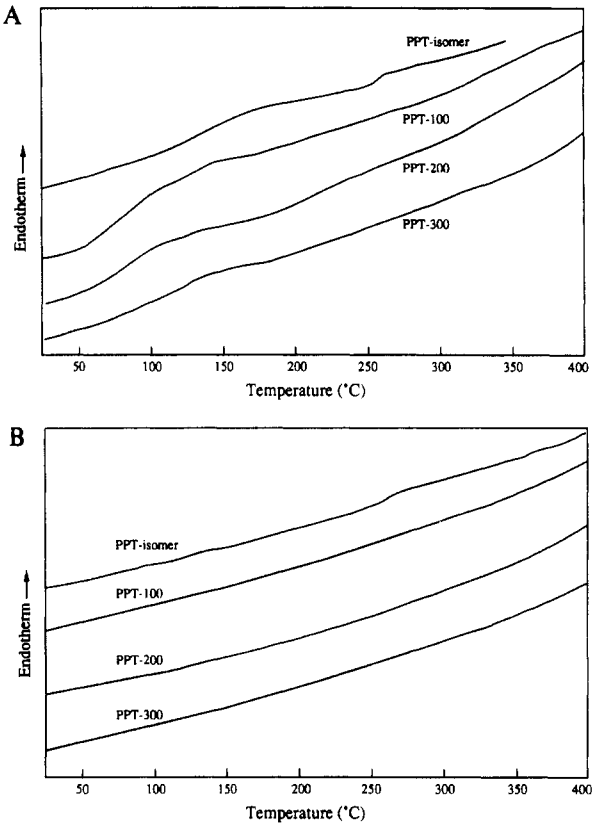

Figure 7. DSC thermograms of the PPT and PPT isomer materials: first scans (a), and second scans (b).

Table I
PPT Film Preparation and Physical Properties

sample	annealing temp, °C	film thickness, mil	density,[a] g/cm^3	density,[b] g/cm^3	% wt loss[c]
PPT isomer		4.35	1.332	1.328	4.2
PPT-100	100	1.05	1.403	1.393	6.4
PPT-200	200	1.08	1.381	1.380	5.3
PPT-300	300	1.07	1.412	1.410	3.8

[a] Measured by aqueous density gradient column at 25 °C. [b] Measured by material bouyancy in nonpolar solutions at room temperature. [c] Percent weight loss in sample by TGA (350 °C vs room temperature).

Table II
Comparison of Oxygen Sorption and Transport Properties at 35 °C in Several Barrier Polymers

sample	X_c	$10^{15}P$, (cm²(STP) cm)/(cm² s cmHg)	$10^{10}D$, cm²/s	10^3S, cm³(STP)/(cm³ atm)
PPT isomer	0	2579	9.26 (9.26)[e]	220 (220)
PPT-100	0.22	220	0.81 (1.04)	220 (282)
PPT-200	0.38	220	1.10 (1.77)	150 (242)
PPT-300	0.45	80	0.62 (1.13)	100 (181)
poly(6-aminohexanoic acid) (Nylon 6)	0.26	1820	39 (56)	35 (47)
poly(*m*-xyleneadipamide) (MXD6)	0.21	773	11 (14)	54 (68)
poly(acrylonitrile) (PAN)[a]	*f*	54	0.14	290
poly(ethylene terephthalate)[b]	0.00	11000	95 (95)	88 (88)
poly(ethylene terephthalate)[b]	0.42	5300	65 (112)	61 (105)
HBA/PET 60/40[c]	*g*	1,100	83	10
HBA/PET 80/20[c]	*g*	500	41	9
Vectra[d]	*g*	47	7	5

[a] Reference 32. [b] Reference 31. [c] Reference 7. [d] Reference 6. [e] Values in parentheses are estimates for the transport coefficients of the noncrystalline regions derived from eqs 2 and 3. [f] PAN has some degree of ordering described as a limited two-phase structure. [g] Thermotropic liquid crystalline materials with estimated X_c values ranging from 5 to 20%.[8]

coefficients. Differences in density among extruded PPT films have been attributed to the existence of microvoids;[13] however, the densities of the PPT samples studied were considerably lower (0.8–1.33 g/cm³) than those used in this investigation (1.38–1.41 g/cm³). The same authors speculated that the density of a partially crystalline PPT sample should be 1.4 g/cm³. Photomicrographs of the cross sections of the PPT films show no evidence of voids. However, a reasonable assessment of the existence microvoids can be gained through analysis of a simple two-phase model for sample density, ρ

$$\frac{1}{\rho} = \frac{X_c}{\rho_c} + \frac{(1 - X_c)}{\rho_{nc}} \tag{6}$$

The density of PPT crystals, ρ_c, has been determined to be 1.48 g/cm³ [12] for both modifications.[14] Using crystallinity levels from X-ray diffraction and the sample densities from the aqueous solution method, the densities of the noncrystalline regions, ρ_{nc}, for the PPT-100, -200 and -300 films were found to be 1.38, 1.33, and 1.36 g/cm³, respectively. Similar analysis of Kevlar 49 fibers (X_c = 0.755, ρ = 1.44 g/cm³) yields a density of 1.33 g/cm³ for the noncrystalline regions. Noncrystalline Nomex fibers have a density of 1.34 g/cm³. For a series of conventional flexible polymers tabulated by Van Krevelen,[30] the average ratio of ρ_{nc} to ρ_c is 0.88. For the PPT materials, the density estimates yield higher ratios ranging from 0.90 to 0.93 suggesting that the noncrystalline phase has a reasonably high density. While the two-phase model has many obvious limitations for the PPT system, these results provide evidence that microvoids are not present.

Gas Transport Results

Comparison with Other Polymers. An important first step in analyzing the transport properties of the PPT films is to compare them with other polymer types as well as the amorphous structural isomer of PPT. In Table II, the oxygen transport coefficients of the PPT films are compared with those of several barrier polymers[31,32] including polyamides and liquid crystalline copolyesters.[6-8] In general, the oxygen permeability coefficients for the PPT films are very low approaching the magnitude of those for PAN (an excellent non-liquid crystalline barrier material)[32,33] and the wholly aromatic liquid crystalline copolyester, Vectra. Oxygen permeability coefficients of the meta-linked PPT isomer are more than 1 order of magnitude higher than those for the crystalline PPT films.

Using reported values for crystallinity in conjunction with eqs 2 and 3, the transport coefficients of the noncrystalline regions of the various materials can be estimated and are listed in parentheses in Table II. Accounting for crystallinity in this manner, the diffusion coefficients for the noncrystalline regions in the PPT materials are still nearly 9 times lower than those for the amorphous isomer. Because of more hindered segmental chain motions, meta-linked aromatic polymers have been shown in numerous instances to have oxygen diffusion coefficients that are from 2 to 6 times lower than those for the para-linked isomer.[19-23] The unusually low diffusivity in the para-linked PPT materials likely results from the fact that the noncrystalline regions are in fact mesomorphic. Because of the well-documented meta versus para linking effect for isotropic amorphous polymers mentioned above, the order of magnitude difference in the PPT and PPT isomer transport behavior most likely underestimates the effect of mesomorphic order. Interestingly, however, the apparent solubility coefficients of the materials are not similarly affected by the ordering of the noncrystalline phase. By correcting for the level of crystallinity, the apparent solubility coefficients of the noncrystalline regions in both the amorphous and mesomorphic materials are very close. These results suggest that the ordering of the noncrystalline regions of the PPT materials strongly inhibits penetrant mobility but has a substantially smaller, if any, effect on sorption capacity. The latter is in strong contrast with observations for mesomorphic copolyesters.[6-8]

With respect to the other polymers in Table II, the oxygen diffusion coefficients of the PPT films are very low, while the solubility coefficients appear to be very high. The diffusion coefficients for the PPT films are 30–40 times lower than those for Nylon 6 and nearly 10 times lower than the partially aromatic MXD6 polyamide material. As discussed earlier, the combination of strong interchain forces and high packing efficiency limit the degree of penetrant mobility. Thus, low diffusivities in the PPT films are expected. The diffusion coefficients of the PPT films are comparable to that for PAN, another material with notably strong interchain forces. The fact that the diffusion coefficients of the PPT materials are considerably lower than those for the liquid crystalline copolyesters may result from the underestimated effects of crystallinity on the diffusion mechanism or it may be an indication of the substantial effects of strong interchain hydrogen-bonding forces. In support of the latter, the diffusion coefficients for the polyamide and PAN materials can be compared with those of the polyesters listed in Table II. Clearly, penetrant mobility in the materials which have strong interchain forces is severely

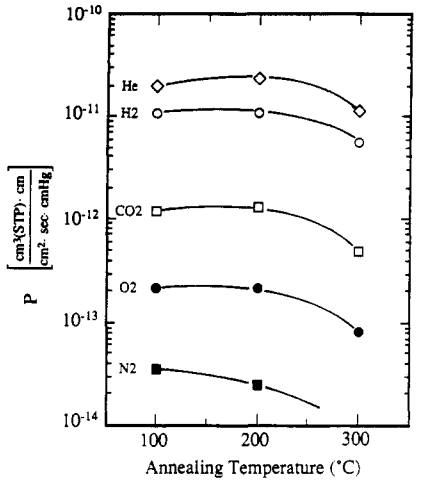

Figure 8. Permeability coefficients of pure gases in the PPT materials at 35 °C as a function of annealing temperature.

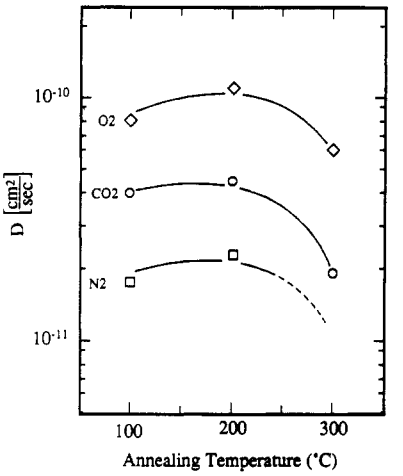

Figure 9. Gas diffusion coefficients for the PPT materials from time-lag data as a function of annealing temperature.

limited in comparison with that in the relatively rigid polyesters.

In contrast with the diffusion coefficients, the solubility coefficients for the PPT materials are surprisingly high. The derived solubility coefficients for the noncrystalline regions of the PPT films are several fold larger than those for Nylon 6, MXD6, and PET but are more comparable to those for PAN and the PPT isomer. However, gas solubility in mesomorphic PPT appears to be nearly 2 orders of magnitude greater than that observed in liquid crystalline copolyester systems.[6-8] In our previous work with various aromatic liquid crystalline copolyesters, mesomorphic order appeared to have an unusually large effect on solubility, while the diffusivity was affected to a lesser degree. The high gas solubility in the PPT materials relative to those for the liquid crystalline copolyesters leads to two possibilities. The first is that the nature of the mesomorphic (but noncrystalline) regions of the PPT films is uniquely different from the mesomorphic structure encountered in the polyester materials in such a way that the sorption capacity is not as dramatically diminished. The second is that the mesomorphic structure in the two systems are similar and that the trends in the solubility coefficients are more directly a consequence of specific differences in chemical structure of the two types of materials. Which of these possibilities is the most dominant will undoubtedly become clearer as more liquid crystalline polymer systems are investigated.

The Effect of Annealing. In Figure 8, the permeability coefficients of the five gases in PPT are plotted as a function of annealing temperature. Like the values for oxygen reported above, the permeability coefficients for the other gases in PPT are also very low. In fact, the nitrogen flux for the PPT-300 sample was below the limits of measurement for the permeation cell employed. New cell designs have been developed which will improve our capabilities for low flux measurements.[34] The trend of permeability with annealing temperature is roughly the same for all of the gases. The permeability coefficients of the samples annealed at 200 °C do not reflect the increase in crystallinity levels as would be expected from eq 2 and 3 but remain nearly the same as those annealed at 100 °C. The permeabilities in samples annealed at 300 °C, however, are 50–60% lower than those annealed at lower temperatures.

The diffusion coefficients for oxygen, nitrogen, and carbon dioxide derived from time-lag data are plotted versus annealing temperature in Figure 9. The time lags for helium and hydrogen were very small, but estimates for D_{He} and D_{H_2} in the PPT films ranged near 8×10^{-8} and 2×10^{-8} cm²/s, respectively. The ratio of the diffusion coefficients for a relatively large gas molecule like oxygen to that of helium in the PPT materials is near 1500. This value can be compared with 2300 for PAN,[32] 1760 for the PPT isomer, 930 for Vectra,[6] 472 for PET,[31] and around 100 for more flexible polymer systems.[1] The high helium to oxygen diffusivity ratio for the PPT samples is clearly consistent with the transport properties of other dense polymer films and with the trends for rigid and strongly interacting chain molecules. Among the PPT films, the larger diffusion coefficients observed in the PPT-200 samples appear to account for its relatively high permeability values. To explain the trend in diffusivities with annealing temperature both the level of crystallinity in the samples and the estimated densities of the noncrystalline regions must be considered. In the case of the PPT-200 film, the low density estimated for the noncrystalline regions is consistent with the relatively high diffusivities, despite the somewhat higher levels of crystallinity, observed for this sample. As discussed, the reasons for the trend in densities among the PPT films are not clear; however, it is apparent that these differences are manifested in penetrant mobility within the polymer matrix.

Effect of Temperature on Transport Coefficients. Transient permeation experiments for carbon dioxide and hydrogen were done over the temperature range 25–60 °C to obtain information about the energetics of transport. The permeability and diffusivity of most polymeric materials[1] including the thermotropic copolyesters[6-8] have been observed to follow an Arrhenius type relationship characteristic of an activated state process. The effect of temperature on the permeation coefficients and diffusion coefficients for PPT films can be seen in Figures 10 and 11, respectively. The Arrhenius parameters for diffusion and permeation in the PPT films and the derived heats of sorption for carbon dioxide are given in Table III. Among the PPT materials, the activation energies and heats of sorption are virtually the same for both meta- and para-linked systems. The differences in absolute diffusion and permeability coefficients among the PPT films are not paralleled by significantly different energetics of transport. In comparison with the values for other conventional polymers, the activation energies of permeation in the PPT films are lower than would be expected for rigid chain polymers with strong interchain forces. The activation energies of diffusion in the PPT systems are more in accord with those for other polymers; however, the values still

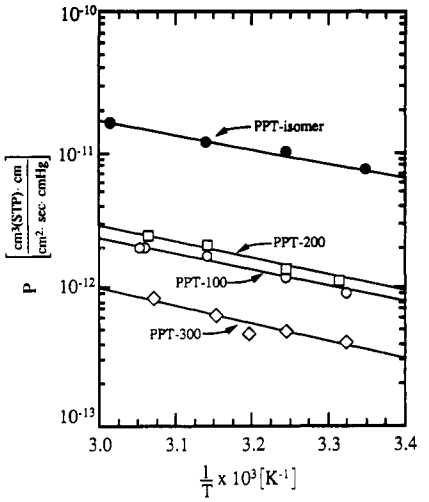

Figure 10. Effect of temperature on the carbon dioxide permeability coefficients for the PPT films.

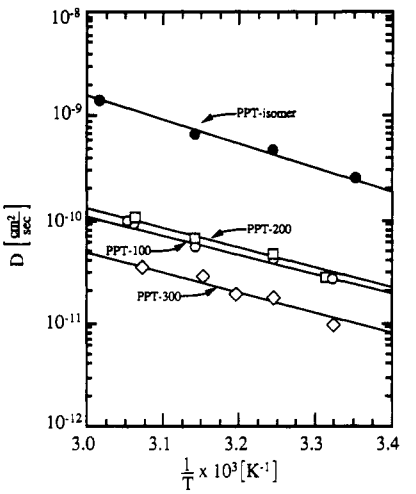

Figure 11. Effect of temperature on the carbon dioxide diffusivity coefficients for the PPT films.

Table III
Arrhenius Parameters and Heats of Sorption for Carbon Dioxide in PPT Films and Other Polymers

sample	E_P, kcal/mol	P_o, barrer	E_D, kcal/mol	D_o, cm²/s	ΔH_S, kcal/mol
PPT isomer	5.5	7.1×10^2	10.5	1.1×10^{-2}	−5.0
PPT-100	5.6	1.1×10^2	9.2	1.3×10^{-4}	−3.6
PPT-200	6.3	4.1×10^2	9.4	1.9×10^{-4}	−3.1
PPT-300	5.9	7.8×10^1	10.1	2.3×10^{-4}	−4.2
Nylon 6	10.0	7.0×10^5	10.9	4.6×10^{-2}	−0.9
MXD6	10.1	3.5×10^5	9.0	4.5×10^{-4}	0.9
PAN[a]	8.1		10.8		−2.7
PET[b]	9.0		11.6		−2.6
Vectra[c]	11.1		13.3		−2.3

[a] Reference 32. [b] Reference 23. [c] Reference 8.

seem low given the extremely low absolute diffusivities reported for these materials. Surprisingly, the activation energies of permeability for hydrogen (E_P = 7.0 kcal/mol) in all of the PPT samples are higher than those for carbon dioxide, suggesting that the low activation energies for CO_2 may be attributed to uniquely strong polymer–penetrant interaction. This strong interaction is evidenced in the largely negative heat of sorption for carbon dioxide in the PPT materials.

Sorption in Kevlar and Nomex Fibers. Transient permeation experiments have led to the conclusion that the mesomorphic regions of the PPT materials have similar solubility coefficients to those observed for the amorphous

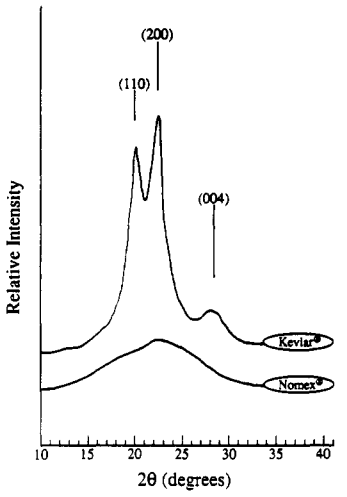

Figure 12. X-ray diffraction patterns of Kevlar 49 and Nomex fibers.

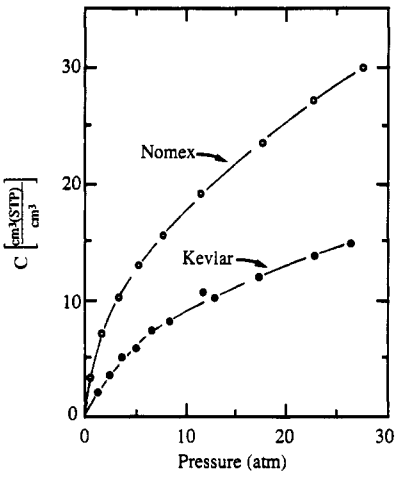

Figure 13. Carbon dioxide sorption isotherms for Kevlar 49 and Nomex fibers at 35 °C.

Table IV
Dual Mode Model Sorption Parameters for CO_2 in Kevlar 49 and Nomex Fibers at 35 °C

sample	k_D, cm³(STP)/(cm² atm)	C_H, cm³(STP)/cm³	b, atm⁻¹
Nomex	0.62	14.2	0.43
Kevlar	0.21	11.5	0.16

PPT isomer. To test this conclusion, static sorption measurements have been performed on Kevlar 49 and Nomex fibers using a pressure decay method commonly used in our laboratory.[27] Because of material availability constraints, the actual amorphous and mesomorphic films could not be tested using this method. As mentioned previously, Nomex fibers are produced from a structural isomer of PPT with a chemical structure similar to that used to make the amorphous films. The X-ray diffraction patterns of samples prepared from finely cut Nomex and Kevlar 49 are given in Figure 12. As with the films prepared from the PPT isomer, the Nomex fibers have no crystalline character. The carbon dioxide sorption isotherms for the Nomex and Kevlar 49 fibers are displayed in Figure 13 along with the parameters (Table IV) obtained by fitting to the dual mode sorption model.[27] The isotherms are

$$C = k_D p + \frac{C'_H b}{1 + bp} p \qquad (7)$$

similar to those of typical glassy polymers such as poly-

carbonate and PET. The Kevlar materials have roughly 50% of the sorption capacity of the amorphous Nomex fibers at any given pressure. Since the estimates for the crystallinity levels in Kevlar 49 fibers are 60–70 vol % (≈65 (this paper) to 75 wt %)[11] and assuming that sorption does not occur in the crystallites, then the sorption isotherm for the noncrystalline regions of the Kevlar materials would fall slightly above that of the Nomex fibers. Clearly, the sorption capacity of the ordered, but noncrystalline regions of the Kevlar fibers is comparable to that of the amorphous Nomex materials. This is consistent with the results from the transient permeation experiments on films made from PPT and the PPT isomer.

Conclusions

From the highly birefringent nature of annealed poly(*p*-phenyleneterephthalamide) (PPT) films, it was apparent that the anisotropy observed in the lyotropic solution (dope) of this polymer was preserved in the solid state. The permeability coefficients of amorphous films prepared from a structural, meta-linked isomer of PPT were much higher than those for the PPT materials. The effects of crystallinity were treated conventionally with simple correlations in an attempt to arrive at values more representative of the transport coefficients of the anisotropic noncrystalline regions of the PPT films. The estimated diffusivities for the mesomorphic regions of the PPT materials are much lower than those observed for the amorphous, meta-linked isomer. However, the apparent solubility coefficients of the amorphous and mesomorphic regions are similar. These sorption characteristics were duplicated in static sorption measurements of carbon dioxide in Kevlar 49 and Nomex fibers and appear to be consistent with the high water sorption capacity observed in Kevlar fibers.[18] Thus, it can be concluded that the ordered, noncrystalline regions of the PPT materials may severly limit penetrant mobility but do not dramatically diminish sorption capacity.

The PPT films exhibited excellent barrier properties approaching those found for polyacrylonitrile and liquid crystalline copolyesters. With respect to other barrier polymers, the transport mechanism in the PPT systems appears to be limited by very low penetrant mobility since solubility coefficients are of the order of typical glassy polymers. Previous investigations with liquid crystalline copolyesters led to the conclusion that mesomorphic order may be the cause for the unusually low solubility of gases observed in these materials. The opposite solubility behavior in the PPT systems could stem from fundamental differences in the mesomorphic order of the noncrystalline regions or from the chemical structure of the two systems. Future studies of liquid crystalline systems with a range of chemical structures is essential to gain a more complete understanding of these solubility differences.

The level of three-dimensional order in the PPT films increased as a function of annealing temperature as evidenced by X-ray diffraction; however, this did not directly translate into lower permeability coefficients for these materials. Despite a substantial increase in the level of crystallinity in the sample annealed at 200 °C, the diffusion coefficients were higher than those observed in the sample annealed at 100 °C. These observations are counter to what would be expected for semicrystalline polymers. The unusual trend in transport coefficients for the PPT films, however, could be closely related to the variation in the density of the materials with annealing.

Acknowledgment. The authors would like to thank Dr. Richard Ubersax of Du Pont for supplying the PPT isomer used in this study. This research was supported by the Separations Research Program of the University of Texas at Austin and by a Phillips Petroleum Co. Foundation fellowship.

References and Notes

(1) Crank, J.; Park, G. S., Eds. *Diffusion in Polymers*; Academic Press: New York, 1968.
(2) Hopfenberg, H. B., Ed. *Permeability of Plastic Films and Coatings to Gases, Vapors, and Liquids*; Plenum Press: New York, 1968.
(3) Michaels, A. S.; Bixler, H. J. *J. Polym. Sci.* **1961**, *50*, 393.
(4) Michaels, A. S.; Parker, R. B., Jr. *J. Polym. Sci.* **1959**, *41*, 53.
(5) Puleo, A. C.; Paul, D. R.; Wong, P. K. *Polymer* **1989**, *30*, 1357.
(6) Chiou, J. S.; Paul, D. R. *J. Polym. Sci.: Polym. Phys. Ed.* **1987**, *25*, 1699.
(7) Weinkauf, D. H.; Paul, D. R. *J. Polym. Sci.: Polym. Phys. Ed.* **1991**, *29*, 329.
(8) Weinkauf, D. H.; Paul, D. R. Submitted to *J. Polym. Sci.: Polym. Phys. Ed.*
(9) E.I. du Pont de Nemours Co., U.S. Pat. 3,869,430, 1974.
(10) Tashiro, K.; Kobayashi, M.; Tadokoro, H. *Macromolecules* **1977**, *10*, 413.
(11) Hindeleh, A. M.; Abdo, Sh. M. *Polymer* **1989**, *30*, 218.
(12) Northholt, M. G. *Eur. Polym. J.* **1974**, *10*, 799.
(13) Bodaghi, H.; Kitao, T.; Flood, J. E.; Fellers, J. F.; White, J. L. *Polym. Eng. Sci.* **1984**, *24*, 242.
(14) Haraguchi, K.; Kajiyama, T.; Takayanagi, M. *J. Appl. Polym. Sci.* **1979**, *23*, 915.
(15) Haraguchi, K.; Kajiyama, T.; Takayanagi, M. *J. Appl. Polym. Sci.* **1979**, *23*, 903.
(16) Roche, E. J.; Allen, S. R.; Gabara, V.; Cox, B. *Polymer* **1989**, *30*, 1776.
(17) Bonner, R. B.; Kohan, M. I.; Lacey, E. M.; Richardson, P. N.; Roder, T. M.; Sherwood, L. T., Jr. *Nylon Plastics*; Kohan, M. I. Ed.; John Wiley and Sons: New York, 1973; Chapter 10.
(18) Fukuda, M.; Kawai, H.; Horii, F.; Kitamaru, R. *Polym. Commun.* **1988**, *29*, 97.
(19) Light, R. R.; Seymour, R. W. *J. Polym. Sci. Eng.* **1982**, *22*, 857.
(20) Sheu, F. R.; Chern, R. T. *J. Polym. Sci.: Polym. Phys. Ed.* **1989**, *27*, 1121.
(21) Stern, S. A.; Mi, Y.; Yamamoto, H. *J. Polym. Sci.: Polym. Phys. Ed.* **1989**, *27*, 1887.
(22) Coleman, M. R.; Koros, W. J. *J. Membr. Sci.* **1990**, *50*, 285.
(23) Aitken, C. L.; Paul, D. R.; Koros, W. J. Paper presented at the International Congress on Membranes and Membrane Processes (ICOM); Chicago, IL, August 1990.
(24) Michaels, A. S.; Bixler, H. J. *J. Polym. Sci.* **1961**, *50*, 413.
(25) Vieth, W.; Wuerth, W. F. *J. Appl. Polym. Sci.* **1969**, *13*, 685.
(26) Petropoulus, J. H. *J. Polym. Sci.: Polym. Phys. Ed.* **1985**, *23*, 1309.
(27) Koros, W. J.; Paul, D. R.; Rocha, A. A. *J. Polym. Sci.: Polym. Phys. Ed.* **1976**, *14*, 687.
(28) Crank, J. *The Mathematics of Diffusion*; Oxford University Press: New York, 1975.
(29) Alexander, L. E. *X-ray Diffraction Methods in Polymer Science*; Wiley: New York, 1969.
(30) Van Krevelen, D. W. *Properties of Polymers*; Elsevier Science Publishers B.V.: Amsterdam, 1990.
(31) Michaels, A. S.; Vieth, W. R.; Barrie, J. A. *J. Appl. Phys.* **1963**, *34*, 13.
(32) Allen, A. H.; Fujii, M.; Stannett, V.; Hopfenberg, H. B.; Williams, J. L. *J. Membr. Sci.* **1977**, *2*, 153.
(33) Frushour, B. G.; Knorr, R. S. In *Handbook of Fiber Science and Technology: Vol. IV, Fiber Chemistry*; Lewin, M., Pearce, E. M., Eds.; Marcel Dekker, Inc.: New York, 1985; Chapter 3.
(34) Weinkauf, D. H. Ph.D. Dissertation, The University of Texas at Austin, 1991.

Registry No. PPT (copolymer), 25035-37-4; PPT (SRU), 24938-64-5; He, 7440-59-7; H_2, 1333-74-0; O_2, 7782-44-7; N_2, 7727-37-9; CO_2, 124-38-9.